

ARTICLE

DOI: 10.1038/s42005-018-0022-7

OPEN

Real-time observation of dissipative soliton formation in nonlinear polarization rotation mode-locked fibre lasers

Junsong Peng¹, Mariia Sorokina², Srikanth Sugavanam², Nikita Tarasov^{2,3}, Dmitry V. Churkin³, Sergei K. Turitsyn^{2,3} & Heping Zeng¹

Formation of coherent structures and patterns from unstable uniform state or noise is a fundamental physical phenomenon that occurs in various areas of science ranging from biology to astrophysics. Understanding of the underlying mechanisms of such processes can both improve our general interdisciplinary knowledge about complex nonlinear systems and lead to new practical engineering techniques. Modern optics with its high precision measurements offers excellent test-beds for studying complex nonlinear dynamics, though capturing transient rapid formation of optical solitons is technically challenging. Here we unveil the build-up of dissipative soliton in mode-locked fibre lasers using dispersive Fourier transform to measure spectral dynamics and employing autocorrelation analysis to investigate temporal evolution. Numerical simulations corroborate experimental observations, and indicate an underlying universality in the pulse formation. Statistical analysis identifies correlations and dependencies during the build-up phase. Our study may open up possibilities for real-time observation of various nonlinear structures in photonic systems.

¹State Key Laboratory of Precision Spectroscopy, East China Normal University, 200062 Shanghai, China. ²Aston Institute of Photonic Technologies, Aston University, Aston Triangle, Birmingham B4 7ET, UK. ³Novosibirsk State University, 1 Pirogova str., Novosibirsk 630090, Russia. Correspondence and requests for materials should be addressed to H.Z. (email: hpzeng@phy.ecnu.edu.cn)

Solitons, localized wave structures formed by the balance between dispersion and nonlinearity, are ubiquitous in nature and are used both as building blocks in theoretical concepts and in various practical applications in many fields of science and engineering, including optics, Bose–Einstein condensates (BEC), hydrodynamics, plasmas, field theory and many others^{1–7}. In addition to fascinating feature of maintaining its shape during propagation, the continuous interest in soliton is also stimulated by their unique properties upon interaction; that is, they behave like particles exerting forces on each other. Interactions between solitons give rise to rich soliton physics, including phenomena such as soliton fusion⁸, fission⁹, full¹⁰ and partial annihilation¹¹, soliton turbulence and many others.

The problem of the soliton formation mechanisms is of a fundamental physical interest. The soliton formation processes are rather different in integrable and non-integrable nonlinear models¹². In the integrable systems, for instance, the Korteweg–de Vries equation, soliton formation process can be periodic (repetitive) when the process is coherently self-seeded and refers to the well-known Fermi–Pasta–Ulam recurrence phenomenon¹³. Such repetitive process can be readily observed in experiments. For instance, periodic pulse collision leading to soliton generation was observed experimentally in a passive fibre ring oscillator¹⁴. In contrast, typical soliton formation dynamics in non-integrable systems is non-repetitive and exhibit complex behaviour before a stationary soliton settles down¹⁵. In contrast to the large number of theoretical studies, experimental observations of soliton build-up dynamics are relatively rare. This is due to the technical difficulties encountered in practice to record such rapid non-repetitive evolution, especially in the realm of ultrafast optical systems, as most of measurement tools only give time-averaged data that washes out these transient dynamics. Recently, through real-time imaging technique, the formation process of matter-wave solitons was captured in BEC⁴. The role of the modulation instability in the solitons formation was elucidated. It is of particular interest to know whether the same mechanism accounts for soliton formation in optics. Formation of extreme optical waves through modulation instability in fibre-optic systems have been studied in Refs^{16,17}.

The term soliton is often used to refer to localized coherent structures in a wide range of nonlinear systems, varying from the integrable (where the term was initially invented) and Hamiltonian systems to non-integrable and non-conservative ones. Many real-world nonlinear systems are non-integrable, meaning the strict mathematic definition of soliton as it was proposed for the integrable systems is rarely met in practice. Therefore, a term 'dissipative soliton' is often used to refer to localized coherent structures in systems with a balance of both conservative effects (e.g. dispersion and nonlinearity) and dissipative ones (gain and loss)^{18–20}. For example, a pulse generated from mode-locked lasers is a dissipative soliton since a laser is intrinsically a dissipative system. Mode-locked lasers provide a flexible platform for studying dissipative soliton dynamics. Recently, by virtue of the emerging real-time measurement technologies such as the time-stretch dispersive Fourier transform (TS-DFT) technique^{21–23} and 'time microscope'^{24,25}, some important dynamics of mode-locked lasers have been unveiled. These studies can be divided into two categories. One relates to repetitive (periodic) processes such as internal motion of soliton molecules^{26,27} and spectral modulation of a single pulse²⁸. The other refers to non-repetitive events such as rogue wave generation^{29–31}, soliton explosions^{32,33} and the build-up of a dissipative soliton/pulse in ultrafast lasers^{34–36}. Various types of soliton interactions may exist during stationary soliton build-up in fibre lasers¹⁵ and are yet to be seen in experiments. Recently, multiple pulsing was observed in the build-up of mode locking in

a Ti: sapphire laser³⁴, the origin of which remains an open question.

In this work, we unveil the build-up of dissipative solitons in mode-locked fibre lasers by means of the TS-DFT technique. We observe two different types of dynamics during dissipative soliton build-up, depending on the length of the laser cavity. In a long cavity, multiple processes are involved in the build-up phase, including modulation instability (Benjamin–Feir instability), mode locking, self-phase modulation (SPM)-induced instability, dissipative soliton splitting and partial annihilation. In a short cavity, only modulation instability and mode locking are responsible for dissipative soliton formation. A long-standing issue in the build-up of mode locking refers to the role of noise involved: a randomly strong noise spike was assumed to evolve to be a mode-locked pulse³⁷. Here we show that the role of noise is to stimulate modulation instability in nonlinear polarization rotation (NPR) mode-locked fibre lasers. We employ advanced statistical analysis to quantify the dependency and correlation between the signals at various stages of dissipative soliton build-up. We show that in complex non-stationary systems correlation and dependency may differ from each other. Thus, their simultaneous application reveal underlying physical processes that can be missed when a simplified analysis is used. Our work shows significant difference to other works^{34–36}. First, modulation instability is firstly unveiled in the initial phase of dissipative soliton formation in our work, in analogy with soliton formation in BEC⁴; second, we observe interference patterns on the transient spectra, evidencing two critical phases: dissipative soliton splitting and interactions of double solitons. These two phases were not observed in other works^{34,35}, as the cavities were short. Soliton interactions were observed in another work³⁶; however, no soliton survived after such interactions, while our work shows that a soliton survives after interactions. The multiple solitons emerged from noisy field³⁶, while double solitons are generated from splitting of a large soliton in our work. It is worth to note that full field measurements of the dissipative solitons are realized in Ref³⁶. Finally, to the best of our knowledge, we firstly present a numerical study on the build-up phase of dissipative soliton in a laser, and show how our numerical study qualitatively agrees with the experiments.

Results

Principle. As a test-bed system, we build a typical dissipative soliton fibre laser as shown in Fig. 1a (see Supplementary Note 1 for details). Since fibre lasers are known to exhibit rich nonlinear dynamics purely by extension of their cavity lengths, the build-up dynamics of dissipative solitons in them are also expected to be different. Hence, the laser cavity length is varied three times during the experiment for a systematic study (see Supplementary Fig. 1 for details). The detection system is shown in Fig. 1b. As shown, the output of the laser is split into two ports by an output coupler. One port (undispersed) is used for measuring the evolution of the instantaneous intensity $I(t)$, over many cavity round-trip (RT) numbers N , in order to produce a two-dimensional spatio-temporal intensity profile $I(t, N)$. The signal from the other port is fed into a long dispersive fibre segment (~11 km here) to stretch the pulses and thus yield spectra measurements (TS-DFT). Two identical photodetectors (PD1, PD2) with 50-GHz bandwidth are used, and the signals are captured by a real-time oscilloscope with bandwidth of 32 GHz (Agilent). It is important to point out that by measuring the temporal delay between the two photodetectors (53.651 μ s), we could conduct simultaneous measurements of the spectral and temporal intensity of the output pulses. The temporal and spectral resolution of the detection system are 30 ps and 0.1 nm, respectively (see Supplementary

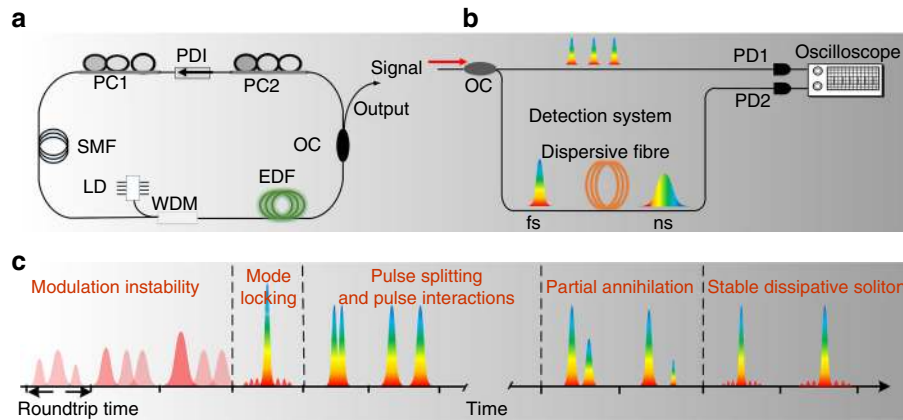


Fig. 1 The build-up of dissipative solitons in a fibre laser with a cavity length of 16 m. **a** The laser setup. LD laser diode, WDM wavelength-division multiplexer, EDF erbium-doped fibre, OC optical coupler, PC polarization controller, PDI polarization-dependent isolator, SMF single-mode fibre. **b** The detection system. PD photodetector. **c** Conceptual representations of different stages during dissipative soliton build-up

Note 2). The accuracy of TS-DFT is confirmed (see Supplementary Fig. 2). The routine to capture the rapid signal during dissipative soliton build-up is as follows. First, by adjusting the polarization controllers (PCs), stable mode-locked lasing is obtained. Next, the pump is switched off, and then the pump is switched on. Upon appearance of a signal, the oscilloscope triggers and records the real-time signal. Although it takes typically several seconds for the pump current to reach the set value, this has no effect on the results since the trigger level is set to be the pulse peak (i.e. the oscilloscope only records data when pulses are formed). Gain relaxation oscillation can also be neglected which has typical time of \sim ms, as here the RT time of the three lasers studied are around 50–100 ns.

Dissipative soliton formation dynamics. We first measure the start-up of dissipative solitons in a fibre laser with cavity length of 16 m. The measured TS-DFT data exhibit drastic changes before a static dissipative soliton is formed (Fig. 2a). Five distinct regimes can be seen in the figure, representing different physical processes involved in the build-up phase (see Fig. 1c for conceptual representation of such phases). During the initial stage of the evolution (up to RT number 100), well-defined intensity patterns (marked by dashed arrows) are presented (Fig. 2a). Since TS-DFT relies on dispersion to stretch pulses, it only works for wide-bandwidth ultra-short pulses, and therefore these intensity patterns represent temporal information of the laser outputs. Such intensity patterns have also been observed in the build-up of mode locking of Kerr-lens mode-locked solid-state lasers³⁴, and are seemingly universal. In fact, these intensity patterns are reminiscent of modulation instability, and we will show that this is indeed the mechanism that gives rise to the observed pattern formations.

On the next stage of the evolution (RTs \sim 100–200), mode locking starts and wide-bandwidth signal (dissipative soliton) is generated, Fig. 2a, the spectra of which can now be measured by TS-DFT. However, this dissipative soliton is not stable and it explodes into soliton molecules (or bound solitons) subsequently, indicated by the modulated spectra (stage 3). Although the spectra seem chaotic from \sim 200 to 350 RTs, modulated structures still exist, and the subsequent spectra (\sim 350–700) show well-defined interference pattern (stage 4). Finally, the spectra are not modulated and keep stable, indicating a stationary dissipative soliton is formed (stage 5). Figure 2b shows typical cross-sections of the spectra at RT numbers of 50, 200, 300, 500 and 800.

The modulated spectra reflect complex temporal evolution of the soliton molecules, which can be revealed by field autocorrelation. It is well known that the Fourier transform of each single-shot spectrum yields a field autocorrelation according to Wiener–Khinchin theorem. Field autocorrelation traces can measure the temporal durations of chirp-free pulses such as dissipative solitons here, but fail to do so for chirped pulses. Nevertheless, they can measure the temporal separations between pulses independent of chirp. As real-time spectra measurement is available by TS-DFT, the field autocorrelation function can be obtained for each RT resolved measurement, where the information about the temporal evolution of the pulses can be recovered. Such a method has been used recently to probe evolving separation between soliton molecules^{26,27}. It is necessary to briefly recall that, if the number of pulses is n , the corresponding peaks of a field autocorrelation trace is $2n-1$. The Fourier transform of each single-shot spectrum in Fig. 2a gives field autocorrelation traces shown in Fig. 2c. It is seen in Fig. 2c that near RT 200 the single peak of the field autocorrelation breaks into three peaks. These reveal that in the corresponding time-domain evolution of the underlying field, the single dissipative soliton explodes to be two. The separation between double dissipative solitons changes quasi-periodically as shown in Box 1 (see Supplementary Fig. 3 for close-up). During later stages of evolution (RT number 400), a third dissipative soliton is formed as indicated by the five peaks of the field autocorrelation function. The separation between the two higher-amplitude dissipative solitons is increased until it reaches a maximum value of 10 ps (Fig. 2c). Beyond this point, the two dissipative solitons start to attract each other, showing decreasing separations between them. They repel each other when the separation reaches its minimum, and only one survives near a RT number 700 as shown in Box 2 (see Supplementary Fig. 3 for close-up), a process which resembles partial annihilation^{10,11}. Figure 2d shows typical cross-sections of the field autocorrelation traces.

It is natural to ask whether the minimum separation is zero or not in Box 2, since zero separation means the two pulses fully overlap. The two dissipative solitons do not fully overlap (see Supplementary Fig. 3 for close-up). Our simulations will also confirm this. We note that this is similar to the scenario of periodic collisions of dispersion-managed solitons, in which the two solitons never fully overlap³⁸. The dynamics of the build-up of a single dissipative soliton under higher pump powers is similar (Supplementary Fig. 4).

It is of significant interest to see whether the build-up phase of dissipative solitons depends on the cavity length of a laser. To this

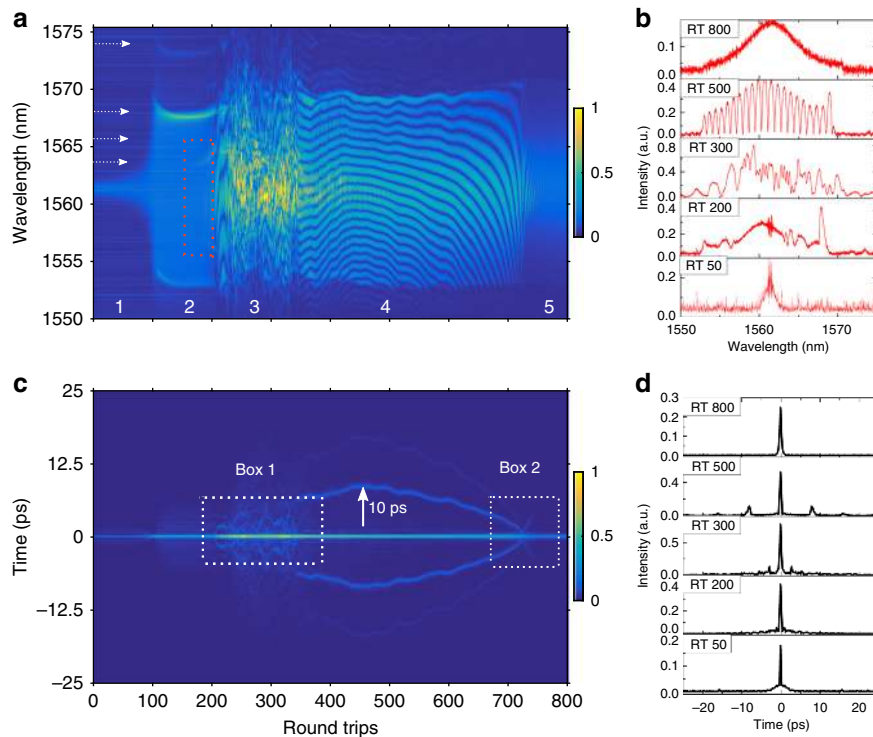


Fig. 2 The experimental results of the build-up of dissipative solitons. **a** The real-time spectral evolution of the laser outputs during dissipative soliton build-up. **b** Typical cross-sections of **a**. **c** The Fourier transforms of each single-shot spectrum in **b** represent the field autocorrelations of the laser outputs, tracing the evolution of temporal separations between dissipative solitons. **d** The representative cross-sections of **c**

end, the length of the laser is varied. In a longer cavity (19.6 m), the essential features (Supplementary Fig. 5) are similar to those observed in the laser described above (Fig. 2). In a shorter laser cavity (10 m), soliton molecules are no longer present in the build-up phase (Supplementary Fig. 6).

Simulations. To provide insight into the laser dynamics during the build-up of dissipative solitons, we performed numerical simulations of the laser based on the nonlinear Schrödinger equation, using a non-distributed model considering every part of the laser (see ‘Methods’). Since nonlinear systems are very sensitive to initial conditions, the build-up dynamics varies significantly for different initial conditions. The diversities are beyond the scope of the current research. Nevertheless, we are able to find the build-up dynamics in simulations which qualitatively agrees with the experimental results by varying the initial conditions. The initial condition used is a weak pulse adding random noise (see Supplementary Fig. 7 for the intensity profile). The results are shown in Fig. 3a; Fig. 3b is the corresponding autocorrelation traces of Fig. 3a. As one can see (Fig. 3a), in the beginning, multiple pulses are formed from the initial conditions. These multiple pulses are generated by modulation instability. The initial conditions contain random noise which effectively seeds modulation instability³⁹. The spectra dynamics also confirm such processes (see Supplementary Fig. 8). For comparison, we performed another simulation in which no noise was added to the initial pulse (therefore modulation instability cannot be triggered), and in this case multiple pulses no longer appear, as expected; the subsequent dynamics is similar to Fig. 3a (Supplementary Fig. 9). We note that multiple pulses were also observed in the build-up of mode locking in solid-state lasers³⁴, the origin of which is still unclear. As nonlinearity and anomalous dispersion are also present in these lasers, those pulses could also be generated by modulation instability.

After modulation instability-induced pulses are generated, the central pulse eventually becomes stronger and only this pulse survives to become a dissipative soliton evident by dispersive wave component in the tail; here mode locking plays an important role in selecting the central pulse and suppressing others, owing to the nature of mode locking which has a larger transmission coefficient for higher-intensity pulses. However, the dissipative soliton is not stable, as indicated by its non-stationary tails (for close-up see Fig. 3c); the origin of such instability caused by SPM will be elaborated later. This instability finally leads to pulse splitting which gives birth to soliton molecules, as shown in the box of Fig. 3a, which is magnified in Fig. 3c. As seen in Fig. 3c, the double dissipative solitons repel each other once they are generated and attraction arises when the separation between them reaches its maximum. However, the pulses cannot fully overlap (merge), similar to experimental observations. The intensity profile of the double pulses (at RT number of 602) with closest separation is shown in the inset of Fig. 3c, and there is no overlap. The pulses repel each other again afterwards. In particular, the leading pulse gets stronger—the trailing one becomes weaker and disappears finally, resulting from the mode-locking mechanism that impose intensity dependent transmission coefficient on the pulses (the weak pulse undergoes higher loss).

Direct soliton–soliton interaction arises from field overlap⁴⁰. The solitons periodically attract and repel each other depending on their initial conditions. In particular, a full overlap (merge) can happen if the two solitons have the same amplitude and meanwhile the relative phase difference is zero. However, a minor difference in the relative amplitude results in a rather different scenario in which the two solitons no longer merge⁴¹. The interactions between solitons are observed in the simulation (Fig. 3c) and above in the experiments (Fig. 2c). Whereas the two pulses exhibit difference in amplitude (Supplementary Fig. 10); therefore, full overlap does not occur.

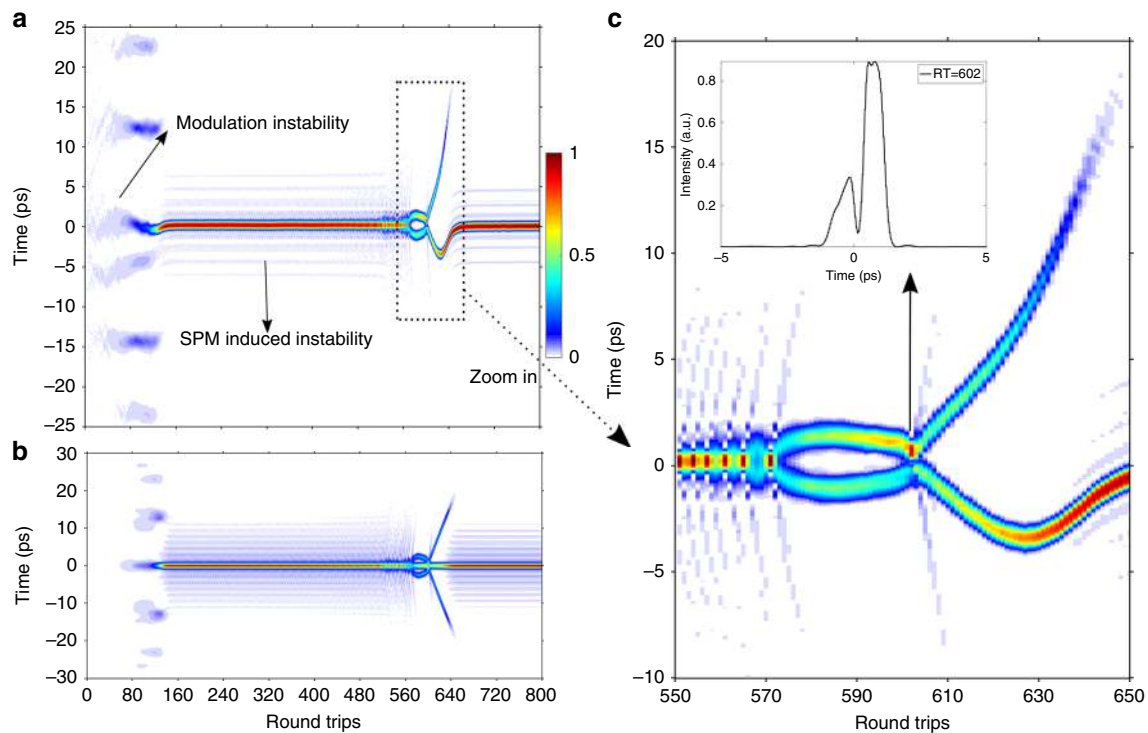


Fig. 3 The build-up of dissipative solitons from simulations. **a** The temporal evolution from the laser outputs. **b** The corresponding autocorrelation trace of **a**. **c** The magnified box in **a** and the inset is the intensity profile of the double dissipative solitons when the distance between them is minimum

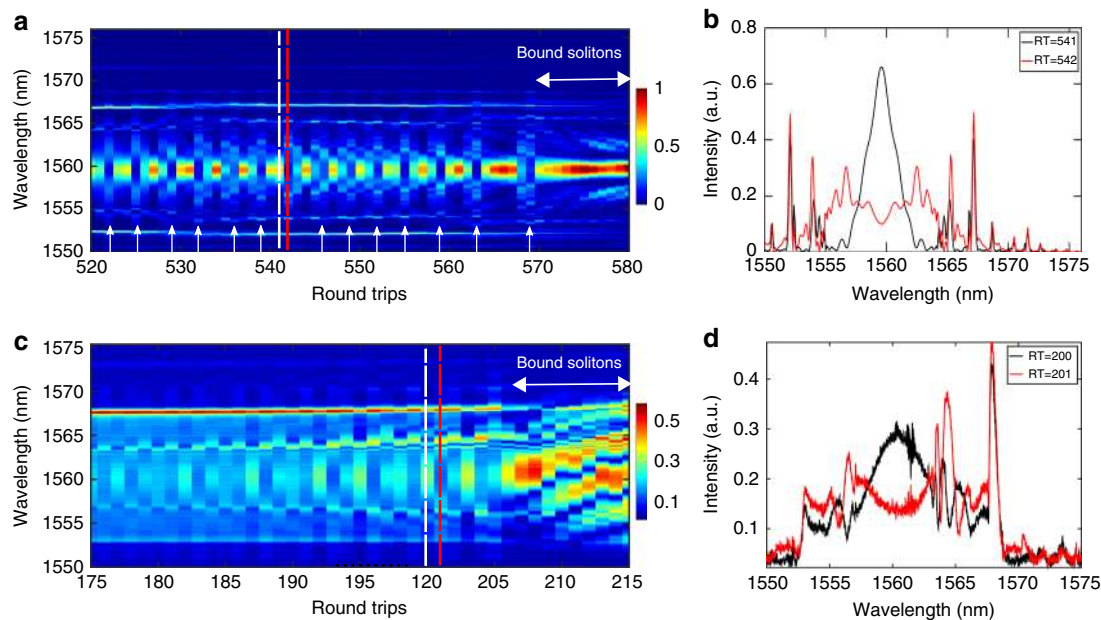


Fig. 4 Instability caused by SPM during the build-up phase of a dissipative soliton. **a** Spectra evolution in the numerical simulations. **b** Two typical consecutive spectra at round-trip (RT) numbers of 541 (black) and 542 (red) in **a**. **c** Spectra evolution measured in the experiments. **d** Two typical consecutive spectra at RT numbers of 200 (black) and 201 (red) in **c**

Further analysis allows us to understand the origin of the instability which leads to dissipative soliton splitting. Such instability can be well understood by investigating its corresponding spectral dynamics. Figure 4a shows the numerically simulated spectra evolution of the non-stationary solitons from 520 to 580 RTs (data corresponds to the data shown on Fig. 3a). It can be seen that quasi-periodic spectral evolution is present, consistent with the temporal evolution. Specifically, the spectra broaden and compress (breath) with drastic changes from one

RT to another (see Fig. 4b). The central spectrum of the dissipative soliton exhibits multiple peaks at an RT number of 542, in contrast to the one at an RT number of 541. These multiple peaks which are weak in the centre and pronounced in the outmost are typical products of SPM⁴¹, indicating that SPM contributes to the observed instability. The arrows in Fig. 4a locate the positions of the SPM-induced broadened spectra. Note that the narrow peaks in the spectrum wings (1550–1555 nm) are Kelly sidebands⁴².

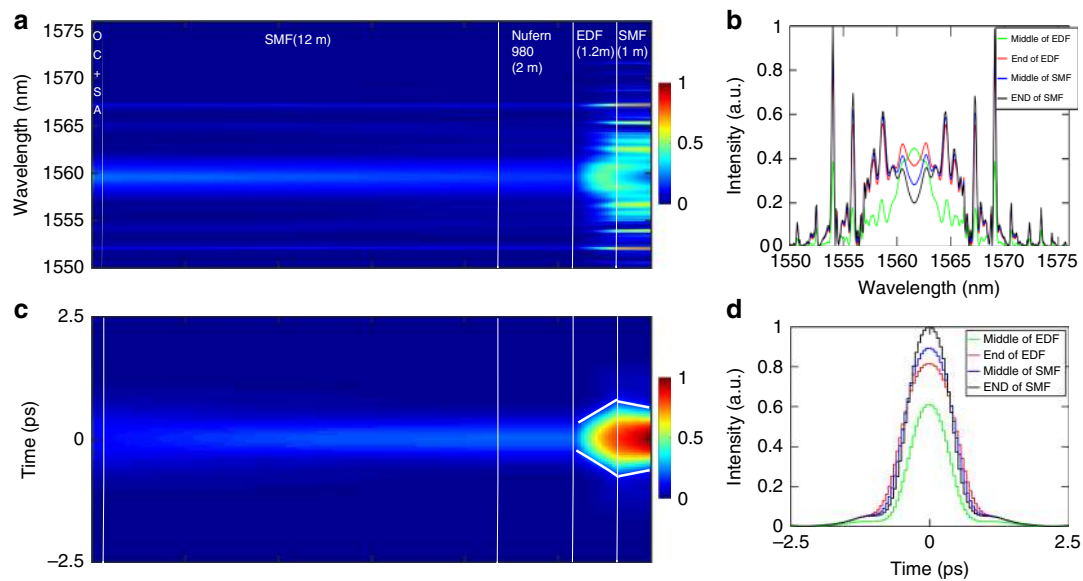


Fig. 5 Intra-cavity evolution of the dissipative soliton from an RT number 541 to 542 in the simulation. **a** The intra-cavity spectral evolution. The intra-cavity components include in turn optical coupler (OC), saturable absorber (SA), single-mode fibre (SMF) (12 m), Nufern 980 fibre (2 m), erbium-doped fibre (EDF) and SMF (1 m). **b** The spectral profiles in the middle (green) and end (red) of the EDF, as well as in the middle (blue) and end (black) of the 1-m SMF following the EDF. **c** The corresponding intra-cavity temporal evolution. **d** The temporal profiles in the middle (green) and end (red) of the EDF, as well as in the middle (blue) and end (black) of the 1-m SMF following the EDF

Experimental observations also show such instability. Figure 4c demonstrates the experimentally measured spectral dynamics (the same data as in Fig. 2a, red box). The quasi-periodic modulation qualitatively agrees with the simulation results. Note that in experiments (Fig. 4d) the SPM effect is not as clear as in numerical simulations, but still takes part in the dissipative soliton dynamics: a nascent dissipative soliton suffers from instability caused by SPM and eventually splits to soliton molecules. Some differences are shown between numerical and experimental results. For instance, the spectra of the bound solitons show asymmetry between the red and blue sides in the experiment (Fig. 4c), which is absent in the simulation. This could be due to third-order dispersion (TOD) which for simplicity is neglected in the simulation, and TOD is well known for inducing spectra asymmetry of pulses⁴³. We stress that the main aim of the numerical analysis is here to validate the different nonlinear processes observed experimentally during the build-up of dissipative soliton including modulation instability, SPM-induced instability, dissipative soliton splitting, transient soliton molecule generation and partial annihilation. Indeed, all these processes are confirmed by the simulation.

It is natural to ask how the dissipative soliton spectrum at an RT number of 541 is shaped to be the one at that of 542 (Fig. 4b). To answer this question, we investigate the intra-cavity evolution of the dissipative soliton (from RTs 541 to 542), revealing that indeed SPM is involved (Fig. 5). The input spectra is the one at an RT of 541, which then propagates inside the laser and is shaped to be the one at an RT of 542. The intra-cavity components include in turn optical coupler (OC), saturable absorber (SA), SMF (12 m), Nufern 980 fibre (2 m) from the pigtailed fibre of the wavelength-division multiplexer, EDF and SMF (1 m). As shown in Fig. 5a, c, the dissipative soliton spectral widths and durations are nearly constant in the SMF (12 m) and Nufern 980 fibre. When the pulse enters the EDF, its spectral and temporal widths are then both broadened; the former is due to amplification and the later results from the normal dispersion of the EDF. After the pulse leaves the EDF, its spectral shape becomes concave around 1560 nm and develops further along the SMF (1 m), as shown in

Fig. 5a, indicating that stronger SPM is present in the SMF. In fact, the concave spectrum already forms in the EDF due to amplification as shown in Fig. 5b (red), while the spectrum is not concave in the middle of the EDF due to lower energy there (Fig. 5b, green). The spectrum becomes more concave as shown in the blue (in the middle of the SMF) and black (end of the SMF) curves in Fig. 5b, due to higher peak power resulting from temporal compression of the dissipative soliton in the SMF, as seen in Fig. 5d where the temporal profiles are shown.

Our experiments and simulations agree qualitatively with each other and reveal the mechanisms of dissipative soliton formation in NPR mode-locked fibre lasers. In contrast to short fibre lasers, long fibre lasers are well known for complex dynamics arising mainly from enhanced nonlinearity. Here we show that the two systems exhibit considerable differences in the build-up of stationary dissipative solitons. In a relatively long laser, first, multiple pulses are generated by modulation instability. Second, mode locking comes to play, which suppresses other pulses and only the central pulse remains. Third, the nascent pulse is not stable, which is evident by its non-stationary spectral evolution due to excessive nonlinearity. Such instability leads to dissipative soliton splitting, giving rise to the generation of soliton molecules. Finally, partial annihilation occurs (only the stronger one survives) since the amplitude of the double pulses are different and this difference is ‘amplified’ by the mode-locking mechanism which imposes higher loss on the weak pulses.

Statistical analysis of dependency and correlation. To investigate an intrinsic dependence and build-up of correlation during pulse propagation, we employ both mutual information and correlation analysis. The concept of mutual information originated from the communication theory and was introduced by C Shannon⁴⁴. It is based on the concept of entropy as a measure of uncertainty–information content associated with the variable. The mutual information in turn gives a quantitative characteristic of the information shared between the variables. Mutual information found applications beyond communications and is actively used in time-series analysis to quantify dependence

between variables^{45,46}. The mutual information is zero when and only when the two variables are independent. This differentiates mutual information from correlation function, as zero correlation does not imply independence. Indeed, mutual information can capture nonlinear or higher-order dependencies, which can be overlooked by analysis of standard correlations⁴⁷.

Here we employ both tools and show when mutual information can provide extra insights not available by using standard correlation analysis. The set of measured DFT data in Fig. 2a can be represented as a set of variables—intensities $I(\lambda, \tau)$, where λ stands for the wavelength and τ describes the RT value. The mutual information between two variables τ_x, τ_y is defined as $MI(\tau_x, \tau_y) = H(\tau_x) + H(\tau_y) - H(\tau_x, \tau_y)$, where $H(\tau) = -\sum p(I(\lambda, \tau)) \ln p(I(\lambda, \tau))$ is the Shannon entropy of the variable and $H(\tau_x, \tau_y)$ is the entropy of a joint set of variables. See Supplementary Note 3 for the calculated mutual information and Pearson's correlations. The most interesting observation, however, is for the stage where mutual information and correlation differ (Supplementary Fig. 11). This highlights complex dynamics and importance of the unstable region on the final soliton solution, which cannot be captured by the correlation function alone.

Discussion

Real-time measurements allow us to access transient fast dissipative soliton dynamics beyond the speed of traditional equipment. We have shown the build-up of dissipative solitons in mode-locked fibre lasers and revealed related nontrivial laser dynamics leading to stable mode-locking regime of a dissipative soliton fibre laser. We find that the nonlinear mechanism of modulation instability leads to the generation of multiple pulses prior to mode locking. Potentially, the same mechanism could attribute to mode-locking build-up in other types of laser systems such as Ti:sapphire laser. Complex laser dynamics is observed during dissipative soliton build-up in a fibre laser with relatively longer cavity, including SPM-induced instability, dissipative soliton splitting, transient soliton molecules and partial annihilation. The experimental observations are confirmed by numerical simulations.

Our study shows that rich nonlinear dynamics can be embedded in nascent evolution of pulses in nonlinear systems. We note that recently universality of the Peregrine soliton formation was demonstrated, during the initial nonlinear evolution stage of high power pulses in fibre⁴⁸. Hence, investigation on nascent stages of pulse evolution in nonlinear systems provides an important way to understand underlying mechanisms governing the dynamics of the systems. On the other hand, we anticipate our work will also stimulate experimental studies of localized structure build-up in other optical systems such as micro-resonators⁴⁹ and semiconductor lasers.

Methods

Pulse propagation within the fibre sections is modelled with a modified nonlinear Schrödinger equation for the slowly varying pulse envelope:

$$\frac{\partial \psi}{\partial z} = -\frac{i}{2} \left(\beta_2 + i \frac{g}{\Omega^2} \right) \frac{\partial^2 \psi}{\partial t^2} + i\gamma |\psi|^2 \psi + \frac{1}{2} g \psi. \quad (1)$$

Here β_2 is the group-velocity delay parameter and γ is the coefficient of cubic nonlinearity for the fibre section. The dissipative terms represent linear gain as well as a Gaussian approximation to the gain profile with the bandwidth Ω . The gain is described by $g = g_0 \exp\left(-\frac{E_p}{E_s}\right)$, where g_0 is the small-signal gain, which is non-zero only for the gain fibre, E_p is the pulse energy and E_s is the gain saturation energy determined by the pump power. To initiate and sustain mode locking of the fibre laser, NPR technique is used in our experiment. Here the mode-locking technique for the sake of clarity is modelled by a simple transfer function:

$$T = R_0 + \Delta R \left(1 - \frac{1}{1 + P/P_c} \right),$$

where R_0 is the unsaturable reflectance, ΔR is the

saturable reflectance, P is the pulse instantaneous power and P_0 is the saturable power. The parameters used in the numerical simulations are similar to their nominal or estimated experimental values (see Supplementary Table 1 for the parameters used). We use this simple model to highlight the main features of the dynamics upon dissipative soliton build-up.

Data availability. The data that support the findings of this study are available from the corresponding author on request.

Received: 28 November 2017 Accepted: 18 April 2018

Published online: 31 May 2018

References

- Mollenauer, L. F., Stolen, R. H. & Gordon, J. P. Experimental observation of picosecond pulse narrowing and solitons in optical fibers. *Phys. Rev. Lett.* **45**, 1095–1098 (1980).
- Turitsyn, S. K., Bale, B. G. & Fedoruk, M. P. Dispersion-managed solitons in fibre systems and lasers. *Phys. Rep.* **521**, 135–203 (2012).
- Kivshar, Y. & Agrawal, G. P. *Optical Solitons: From Fibers to Photonic Crystals* (Academic, New York, 2003).
- Nguyen, J. H. V., Luo, D. & Hulet, R. G. Formation of matter-wave soliton trains by modulational instability. *Science* **356**, 422–426 (2017).
- Kuznetsov, E., Rubenchik, A. & Zakharov, V. E. Soliton stability in plasmas and hydrodynamics. *Phys. Rep.* **142**, 103–165 (1986).
- Stegeman, G. I. & Segev, M. Optical spatial solitons and their interactions: universality and diversity. *Science* **286**, 1518–1523 (1999).
- Yang, Y. *Solitons in Field Theory and Nonlinear Analysis* (Springer, New York, 2001).
- Shih, M.-F. & Segev, M. Incoherent collisions between two-dimensional bright steady-state photorefractive spatial screening solitons. *Opt. Lett.* **21**, 1538–1540 (1996).
- Krölikowski, W. & Holmstrom, S. A. Fusion and birth of spatial solitons upon collision. *Opt. Lett.* **22**, 369–371 (1997).
- Krölikowski, W., Luther-Davies, B., Denz, C. & Tschudi, T. Annihilation of photorefractive solitons. *Opt. Lett.* **23**, 97–99 (1998).
- Descalzi, O., Cisternas, J., Escaff, D. & Brand, H. R. Noise induces partial annihilation of colliding dissipative solitons. *Phys. Rev. Lett.* **102**, 188302 (2009).
- Rumpf, B. & Newell, A. C. Coherent structures and entropy in constrained, modulationally unstable, nonintegrable systems. *Phys. Rev. Lett.* **87**, 054102 (2001).
- Zabusky, N. J. & Kruskal, M. D. Interaction of 'Solitons' in a collisionless plasma and the recurrence of initial states. *Phys. Rev. Lett.* **15**, 240–243 (1965).
- Wu, M. & Patton, C. E. Experimental observation of Fermi–Pasta–Ulam recurrence in a nonlinear feedback ring system. *Phys. Rev. Lett.* **98**, 047202 (2007).
- D'yachenko, A. I., Zakharov, V. E., Pushkarev, A. N., Shvets, V. F. & Yan'kov, V. V. Soliton turbulence in nonintegrable wave systems. *Sov. Phys. JETP* **69**, 1144–1147 (1989).
- Kibler, B. et al. The Peregrine soliton in nonlinear fibre optics. *Nat. Phys.* **6**, 790–795 (2010).
- Dudley, J. M., Dias, F., Erkintalo, M. & Genty, G. Instabilities, breathers and rogue waves in optics. *Nat. Photon.* **8**, 755–764 (2014).
- Picholle, E., Montes, C., Leycuras, C., Legrand, O. & Botineau, J. Observation of dissipative superluminescent solitons in a Brillouin fiber ring laser. *Phys. Rev. Lett.* **66**, 1454–1457 (1991).
- Vanin, E. V. et al. Dissipative optical solitons. *Phys. Rev. A* **49**, 2806–2811 (1994).
- Grelu, P. & Akhmediev, N. Dissipative solitons for mode-locked lasers. *Nat. Photon.* **6**, 84–92 (2012).
- Goda, K. & Jalali, B. Dispersive Fourier transformation for fast continuous single-shot measurements. *Nat. Photon.* **7**, 102–112 (2013).
- Mahjoubfar, A. et al. Time stretch and its applications. *Nat. Photon.* **11**, 341–351 (2017).
- Runge, A., Aguerregaray, C., Broderick, N. & Erkintalo, M. Coherence and shot-to-shot spectral fluctuations in noise-like ultrafast fiber lasers. *Opt. Lett.* **38**, 4327–4330 (2013).
- Suret, P. et al. Single-shot observation of optical rogue waves in integrable turbulence using time microscopy. *Nat. Commun.* **7**, 13136 (2016).
- Närhi, M. et al. Real-time measurements of spontaneous breathers and rogue wave events in optical fibre modulation instability. *Nat. Commun.* **7**, 13675 (2016).

26. Herink, G., Kurtz, F., Jalali, B., Solli, D. R. & Ropers, C. Real-time spectral interferometry probes the internal dynamics of femtosecond soliton molecules. *Science* **356**, 50–54 (2017).
27. Krupa, K., Nithyanandan, K., Andral, U., Tchofo-Dinda, P. & Grelu, P. Real-time observation of internal motion within ultrafast dissipative optical soliton molecules. *Phys. Rev. Lett.* **118**, 243901 (2017).
28. Li, B. et al. Real-time observation of round-trip resolved spectral dynamics in a stabilized fs fiber laser. *Opt. Exp.* **25**, 8751–8759 (2017).
29. Solli, D. R., Ropers, C., Koonath, P. & Jalali, B. Optical rogue waves. *Nature* **450**, 1054–1057 (2007).
30. Lecaplain, C., Grelu, P., Soto-Crespo, J. & Akhmediev, N. Dissipative rogue waves generated by chaotic pulse bunching in a mode-locked laser. *Phys. Rev. Lett.* **108**, 233901 (2012).
31. Peng, J., Tarasov, N., Sugavanam, S. & Churkin, D. V. Rogue waves generation via nonlinear soliton collision in multiple-soliton state of a mode-locked fiber laser. *Opt. Exp.* **24**, 21256–21263 (2016).
32. Soto-Crespo, J., Akhmediev, N., & Ankiewicz, A. Pulsating, creeping, and erupting solitons in dissipative systems. *Phys. Rev. Lett.* **85**, 2937–2940 (2000).
33. Runge, A. F., Broderick, N. G. & Erkintalo, M. Observation of soliton explosions in a passively mode-locked fiber laser. *Optica* **2**, 36–39 (2015).
34. Herink, G., Jalali, B., Ropers, C. & Solli, D. R. Resolving the build-up of femtosecond mode-locking with single-shot spectroscopy at 90 MHz frame rate. *Nat. Photon.* **10**, 321–326 (2016).
35. Wei, X. et al. Unveiling multi-scale laser dynamics through time-stretch and time-lens spectroscopies. *Opt. Exp.* **25**, 29098–29120 (2017).
36. Ryczkowski, P. et al. Real-time measurements of dissipative solitons in a mode-locked fiber laser. *Nat. Photon.* <https://www.nature.com/articles/s41566-018-0106-7> (2018).
37. Keller, U. Recent developments in compact ultrafast lasers. *Nature* **424**, 831–838 (2003).
38. Roy, V., Olivier, M., Babin, F. & Piché, M. Dynamics of periodic pulse collisions in a strongly dissipative-dispersive system. *Phys. Rev. Lett.* **94**, 203903 (2005).
39. Solli, D. R., Herink, G., Jalali, B. & Ropers, C. Fluctuations and correlations in modulation instability. *Nat. Photon.* **6**, 463–468 (2012).
40. Gordon, J. Interaction forces among solitons in optical fibers. *Opt. Lett.* **8**, 596–598 (1983).
41. Agrawal, G. P. *Nonlinear Fiber Optics* (Academic, New York, 2007).
42. Kelly, S. Characteristic sideband instability of periodically amplified average soliton. *Electron. Lett.* **28**, 806–807 (1992).
43. Kalashnikov, V. L., Sorokin, E., Naumov, S. & Sorokina, I. T. Spectral properties of the Kerr-lens mode-locked Cr4+:YAG laser. *J. Opt. Soc. Am. B* **20**, 2084–2092 (2003).
44. Shannon, C. E. A mathematical theory of communication. *Bell Syst. Tech. J.* **27**, 379–423, 623–656 (1948).
45. Dionisio, A., Menezes, R. & Mendes, D. A. Mutual information: a measure of dependency for nonlinear time series. *Phys. A* **344**, 326–329 (2004).
46. Sugavanam, S., Sorokina, M. & Churkin, D. V. Spectral correlations in a random distributed feedback fibre laser. *Nat. Commun.* **8**, 15514 (2017).
47. Li, W. Mutual information functions versus correlation functions. *J. Stat. Phys.* **60**, 823–837 (1990).
48. Tikan, A. et al. Universality of the Peregrine soliton in the focusing dynamics of the cubic nonlinear Schrödinger equation. *Phys. Rev. Lett.* **119**, 033901 (2017).
49. Herr, T. et al. Mode spectrum and temporal soliton formation in optical microresonators. *Phys. Rev. Lett.* **113**, 123901 (2014).

Acknowledgements

We acknowledge the support from National Natural Science Fund of China (11434005, 11621404, 11561121003, 61775059 and 11704123) and the Russian Science Foundation (grant no. 17-72-30006). D. V. C. is supported by Ministry of Education and Science of the Russian Federation (project 14.Y26.31.0017).

Author contributions

J.P. performed the experiments. S.S. and J.P. measured the delay between temporal and spectral measurements. N.T. and S.S. provided early-stage assistance in spatio-temporal intensity measurements. J.P. and H.Z. carried out numerical simulations. M.S. and S.K.T. conceived the idea of studying the soliton formation from noise by using mutual information and correlation analysis. M.S. did the statistical analysis and wrote the corresponding section of the manuscript. H.Z., D.V.C. and S.K.T. supervised and guided the project. All authors contributed to the writing of the paper.

Additional information

Supplementary Information accompanies this paper at <https://doi.org/10.1038/s42005-018-0022-7>.

Competing interests: The authors declare no competing interests.

Reprints and permission information is available online at <http://npg.nature.com/reprintsandpermissions/>

Publisher's note: Springer Nature remains neutral with regard to jurisdictional claims in published maps and institutional affiliations.



Open Access This article is licensed under a Creative Commons Attribution 4.0 International License, which permits use, sharing, adaptation, distribution and reproduction in any medium or format, as long as you give appropriate credit to the original author(s) and the source, provide a link to the Creative Commons license, and indicate if changes were made. The images or other third party material in this article are included in the article's Creative Commons license, unless indicated otherwise in a credit line to the material. If material is not included in the article's Creative Commons license and your intended use is not permitted by statutory regulation or exceeds the permitted use, you will need to obtain permission directly from the copyright holder. To view a copy of this license, visit <http://creativecommons.org/licenses/by/4.0/>.

© The Author(s) 2018